Surface & Coatings Technology 231 (2013) 346–352

Contents lists available at ScienceDirect

Surface & Coatings Technology

journal homepage: www.elsevier.com/locate/surfcoat

Toward hard yet tough CrAlSiN coatings via compositional grading

Yu Xi Wang [a], Sam Zhang [a,*], Jyh-Wei Lee [b], Wen Siang Lew [c], Deen Sun [d], Bo Li [e]

[a] School of Mechanical and Aerospace Engineering, Nanyang Technological University, 50 Nanyang Avenue, Singapore 639798, Singapore
[b] Center for Thin Film Technologies and Applications, Mingchi University of Technology, Taipei 24301, Taiwan
[c] School of Physical and Mathematical Sciences, Nanyang Technological University, 21 Nanyang Link, Singapore 637371, Singapore
[d] PVD Department Plating Division, Singapore Epson Industrial Pte Ltd, Singapore 628162, Singapore
[e] Central Iron and Steel Research Institute, Beijing 100081, P.R. China

ARTICLE INFO

Available online 17 March 2012

Keywords:
CrAlSiN
Gradient structure
Toughness
Magnetron sputtering

ABSTRACT

A set of CrAlSiN coatings was synthesized in homogenous and graded composition via magnetron sputtering in mixed Ar and N_2 ambient. The microstructures are investigated using glancing angle X-ray diffractometry, field emission scanning electron microscopy and transmission electron microscopy. With compositional grading, CrAlSiN coatings exhibit much improved scratch adhesion strength and better crack propagation resistance at a little expense of hardness.

© 2012 Elsevier B.V. All rights reserved.

1. Introduction

In recent years, CrAlN protective coatings have been considered promising for their enhanced corrosion and oxidation resistance as well as higher hardness [1–3]. With the addition of Si, the thermal stability of the coating is improved [4–6].

In addition to compositional modification, another approach to achieve multifunctionality is dedicated tailoring of the coating architecture through multilayering [7] or grading [8]. Hardness and oxidation resistance are improved with multilayer structure [9,10]. Compositional [11] and/or structural grading [12], on the other hand, have been proven effective in reducing crack concentration and improving the adhesion between coatings and substrate. For practical engineering applications, it is much more important to have a combination of high toughness with reasonably high hardness, rather than super high in hardness but brittle. High toughness means high resistance to crack formation under stress, in other words, high energy absorption to deter crack propagation. Hard yet tough coatings are much desired but difficult to come by [13] and it is aimed in this paper that the hard yet tough CrAlSiN coatings can be achievable through compositional Si grading.

Current investigation targets toughness enhancement through compositional grading of Si to form CrAlSiN coatings. Scratch crack propagation resistance (CPR_s) [14] measurements indicate that the compositional grading of Si gives rise to better toughness while maintaining adequate hardness. In addition, X-ray photoelectron spectroscopy, electron probe micro-analyzer, glow discharge optical emission spectroscopy, glancing angle X-ray diffractometry, field emission scanning electron microscopy and transmission electron microscopy have been employed for a detailed composition and microstructure characterization of the coating as a function of Si addition.

2. Experiment setup

The deposition of the coatings was conducted via co-sputtering of Cr (6 in. in dia., 99.99% in purity), Al (6 in. in dia., 99.99% in purity) and Si (6 in. in dia., 99.99% in purity) targets on Si (100) wafer and mirror-finishing stainless steel 420 (SUS420) disks in mixed Ar and N_2 ambient. All the targets were mounted ~150 mm above the substrate. The base pressure in the deposition chamber was pumped better than 5.0×10^{-5} Pa and the processing pressure was maintained at 0.4 Pa at Ar flow rate of 40 sccm and N_2 of 20 sccm. During the deposition, the substrate temperature was kept at 400 °C. The configuration of applied power is listed in Table 1. The substrate holder was allowed to rotate steadily in order to guarantee the homogeneous feature along the surface plane. Compositional grading of Si was realized through gradual step-wise increase of the power on the Si target. Two series of grading were prepared: the power density on Si target varied from 0 to 2.74 W/cm^2 (increasing step of 0.22 W/cm^2/10 min) and that on Si target from 0 to 4.11 W/cm^2 (increasing step of 0.275 W/cm^2/10 min). A series of CrAlSiN coatings with different Si addition (from 0 to 8.5 at.%) were also prepared as the counterparts. The radio frequency (r.f.) induced negative bias voltage was set at −160 V. The total thickness of film was controlled at around 1 μm. Before deposition took place, a 15 min plasma etching was conducted at negative bias voltage (r.f.) of −160 V to remove oxides and contaminants that may still cling on the surface.

The bonding states of Cr, Al, N and Si were characterized using X-ray photoelectron spectroscopy (XPS, Kratos AXIS Ultra). The composition of CrAlSiN coatings was evaluated using Field Emission

* Corresponding author. Tel.: +65 67904400; fax: +65 67911859.
E-mail address: MSYZHANG@ntu.edu.sg (S. Zhang).

0257-8972/$ – see front matter © 2012 Elsevier B.V. All rights reserved.
doi:10.1016/j.surfcoat.2012.03.036

Table 1
Power on target, chemical concentration, hardness, Young's modulus, roughness and critical load of as-deposited coatings.

Code	Power on target (W)			Concentration (at.%)					H (GPa)	E (GPa)	R_a	L_{C1} (N)	L_{C2} (N)
	Cr	Al	Si	Cr	Al	Si	N	O					
CrAlN	400	600	0	28.5	17.4	0	52.6	1.5	12.7 ± 2.0	261 ± 15	15.1	15.0	36.8
CrAlSiN-1	400	600	250	28.6	17.6	0.4	51.9	1.5	10.9 ± 1.5	258 ± 20	13.9	23.6	43.6
CrAlSiN-2	400	600	500	26.7	16.8	1.8	53.6	1.2	12.4 ± 2.1	298 ± 33	13.7	9.6	27.5
CrAlSiN-3	400	600	750	23.4	15.6	5.9	53.8	1.3	19.3 ± 2.9	263 ± 7	6.6	9.2	28.2
CrAlSiN-4	267	400	750	21.4	13.5	8.5	55.2	1.4	29.5 ± 0.6	303 ± 6	0.9	3.7	13.6
CrAlSiN-GL[a]	400	600	0–750	25.5	15.9	2.9	54.3	1.4	15.2 ± 2.5	319 ± 31	11.3	13.6	38.6
CrAlSiN-GH[a]	267	400	0–750	25.9	16.5	3.2	53.2	1.2	25.9 ± 2.5	320 ± 21	9.2	6.8	23.2

[a] Average value throughout the coating.

Electron Probe Micro-Analyzer (FE-EPMA, JEOL JXA-8500F) with the aid of the ZAF-corrected program. The accelerating voltage was 12 kV to achieve a detection depth of around 1 μm. The composition distribution of graded CrAlSiN coatings was characterized using Glow Discharge Optical Emission Spectroscopy (GDOES, GD Profiler 2, HORIBA JOBIN YVON) calibrated from the referenced homogenous CrAlSiN coatings with known compositions.

The crystalline structure was analyzed using Glancing Angle X-ray Diffractometry (GAXRD, Panalytical X'Pert Pro) with a Cu-Kα 40 kV/30 mA X-ray source (wavelength λ = 0.15406 nm). The glancing incident was set at 1° at the step size of 0.05°.

The cross-sectional microstructure was investigated using Field Emission Scanning Electron Microscopy (FESEM, JEOL JSM-6701F) and Transmission Electron Microscopy (TEM, JEOL JEM-2100F). The

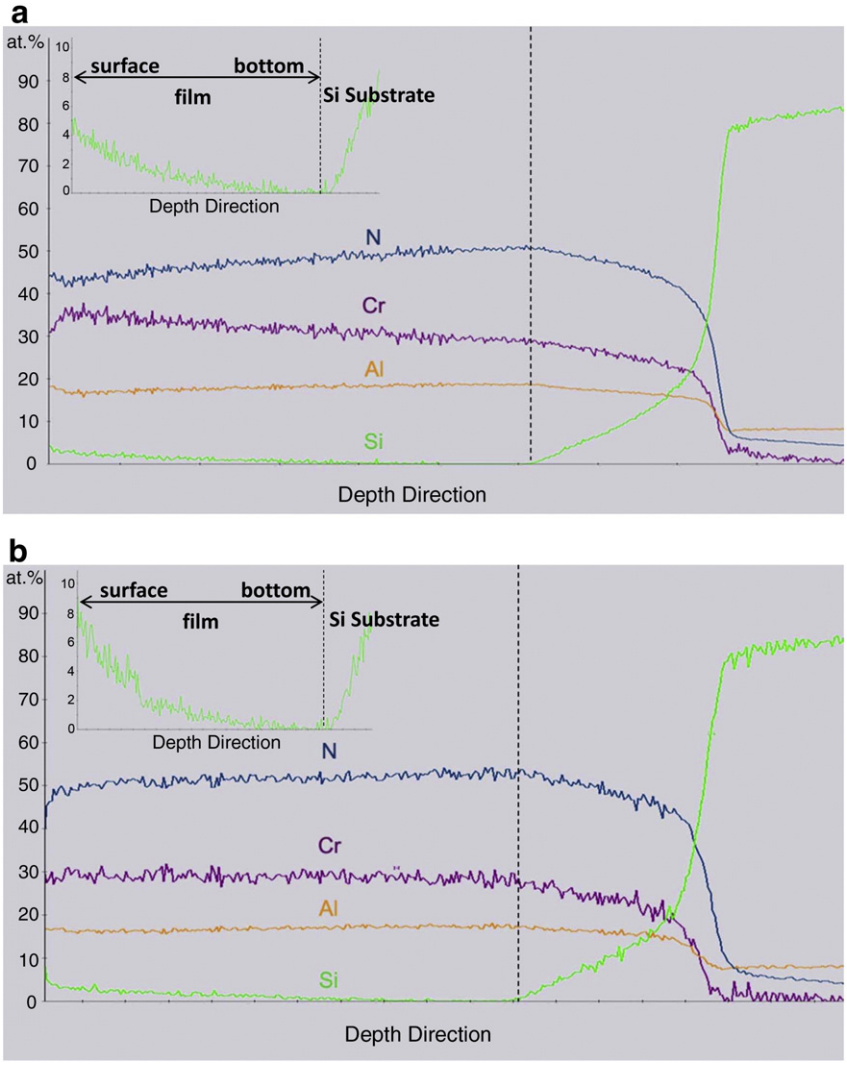

Fig. 1. GDOES results of (a) CrAlSiN-GL (b) CrAlSiN-GH, inset is the enlarged Si curve.

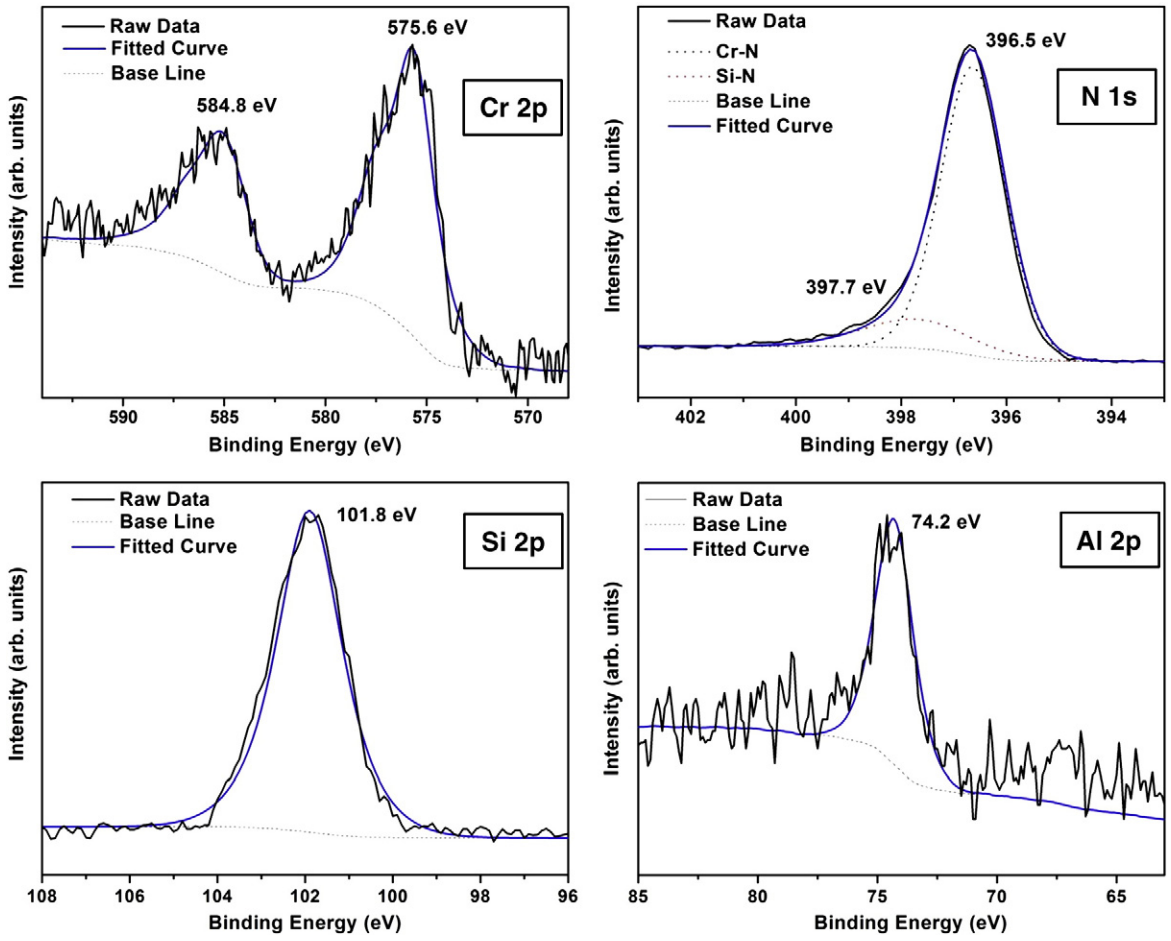

Fig. 2. XPS core-level spectra of Cr 2p, N 1s, Si 2p, Al 2p.

arithmetical mean of surface roughness (R_a) was obtained using an Atomic Force Microscopy (AFM, Vecco Dimension 3000) operated under the tapping mode (resolution of 512 pixels × 512 pixels in $10 \times 10\ \mu m^2$ area at scanning frequency of 1.0 Hz).

Hardness and Young's modulus were measured using a nanoindenter (Hysitron TI-900 TriboIndenter). Maximum indentation depth was set at 80 nm, less than one tenth of the coating thickness to minimize the substrate effect. To get the reliable mean value and standard deviation, at least 8 points for each sample were tested.

Crack resistance was evaluated through a micro-scratch test (J&L Tech. Scratch Tester) on coatings deposited on SUS420 substrate. Applied linear load was set from 0 to 50 N. The scanning length was set at 5 mm with a scanning speed of 0.08 mm/s. For each sample, 3 times scratch tests were carried out to obtain the average load of L_{C1} and L_{C2}.

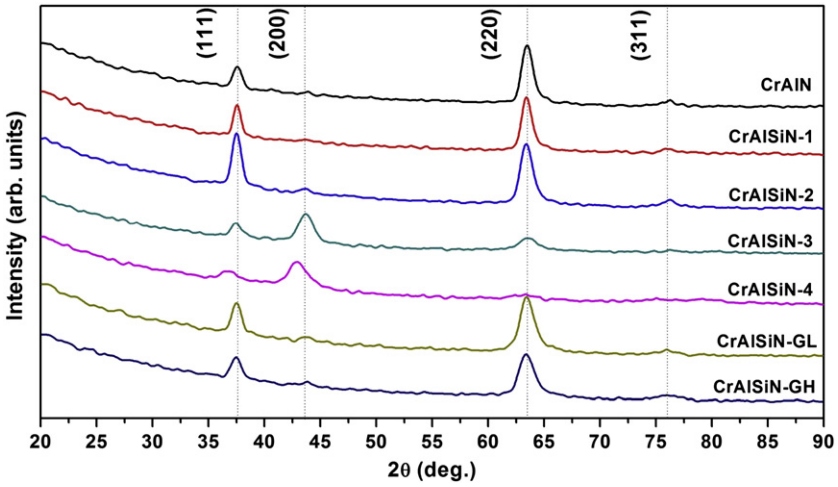

Fig. 3. GAXRD patterns of as-deposited CrAlSiN coatings.

3. Results and discussion

3.1. Chemical composition and bonding state

Table 1 summarizes the chemical composition as determined by EPMA analysis. As the electron penetration is about coating thickness in EPMA, the chemical composition in the graded CrAlSiN coatings is determined as an average throughout the coatings. Typical GDOES depth profiles for the coatings on the Si substrate are plotted in Fig. 1, where Si distribution on thickness is observed as expected: almost 0 at the substrate to ~5 at.% on top surface of CrAlSiN-GL (Fig. 1(a)) and to ~8 at.% on top surface of CrAlSiN-GH (Fig. 1(b)). As shown in Fig. 1, Si decreases from the top to the bottom, indicating the gradual distribution. The increased composition of Si and decreased of other elements is regarded that the detected area is the Si substrate.

The narrow scanned XPS results were taken representatively from the CrAlSiN-4, (Fig. 2). Cr $2p_{3/2}$ and Cr $2p_{1/2}$ are observed at 575.6 eV and 584.8 eV, respectively, corresponding to Cr – N bonding. The N 1s peak reveals two different chemical features: the one centered at 396.5 eV is for Cr – N bond and the one at 397.7 eV is for Si – N bond [15]. The Si 2p spectrum is for Si – N bonding at 101.8 eV. The Al 2p spectrum shows a characteristic peak at 74.2 eV for Al – N bonding [15]. It should be pointed out that the added Si only affects the amount of Si – N bonds without significant influence on the bonding state.

3.2. Crystalline structure

The X-ray diffraction patterns of as-deposited coatings are presented in Fig. 3. B1 NaCl-type fcc structure is confirmed from the diffraction peaks of (111), (200), (220) and (311). For the homogenous structure coatings, peaks become broadening with increased intensity on (200) as Si content increases. And no peaks corresponding to crystalline silicon nitride can be identified. Together with the results of XPS, it is concluded that the added Si leads to the formation of amorphous SiN_x. Peak broadening indicates the formation of fine-grained structure, while the variation of orientation is attributed to the minimization of the total energy during film deposition. Similar results were also reported by Chen et al. [4,5]. With increase of Si content, segregated amorphous SiN_x would interrupt the preferable growth of (111) plane, leading to the discontinuous growth of nitride grains, thus the intrinsic stress and strain energy no longer dominates the orientation. In consequence, the grains grow along the (200) to achieve the lowest surface energy. It should be noted that obvious peaks shift toward small diffraction angle is observed at higher Si content (CrAlSiN-3 and CrAlSiN-4). This is correspondence with previous study by Barshilia et al. [16]. For the graded coatings, the diffraction patterns are similar with that of homogenous coatings with low level of Si addition (CrAlSiN-1 and CrAlSiN-2). This is attributed to the composition distribution that the dominant fraction of graded coatings (mediate and lower layer) is of low Si addition which favor the growth orientation in [111] and [220] direction.

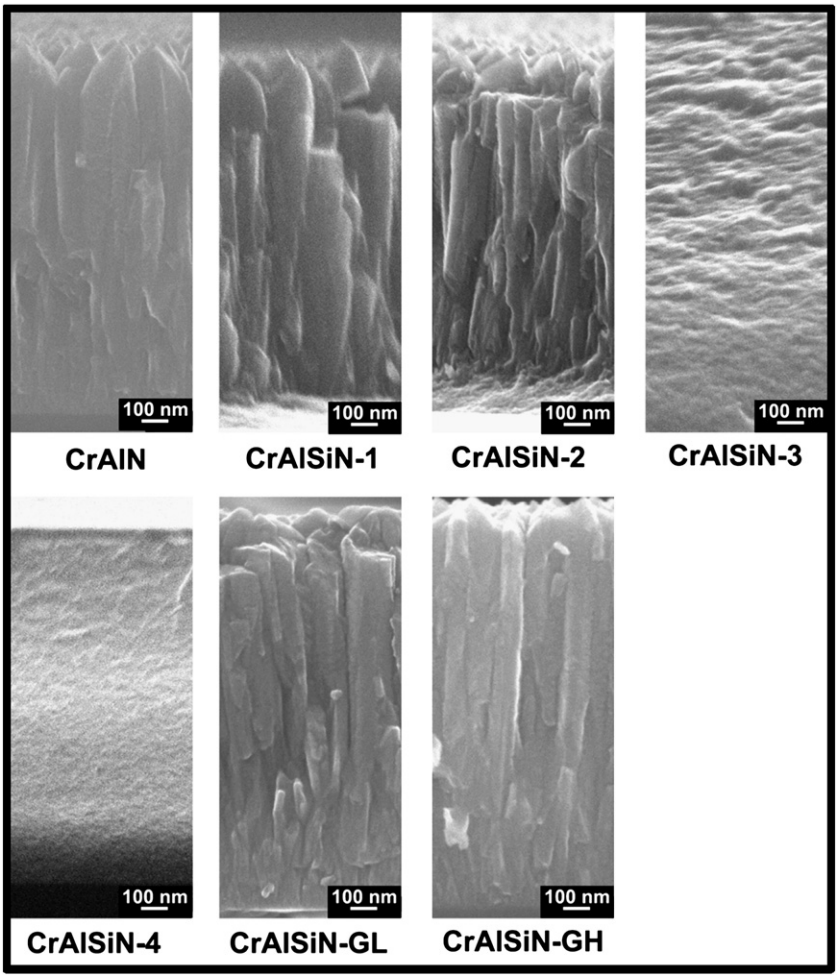

Fig. 4. Cross-sectional morphology of as-deposited CrAlSiN coatings.

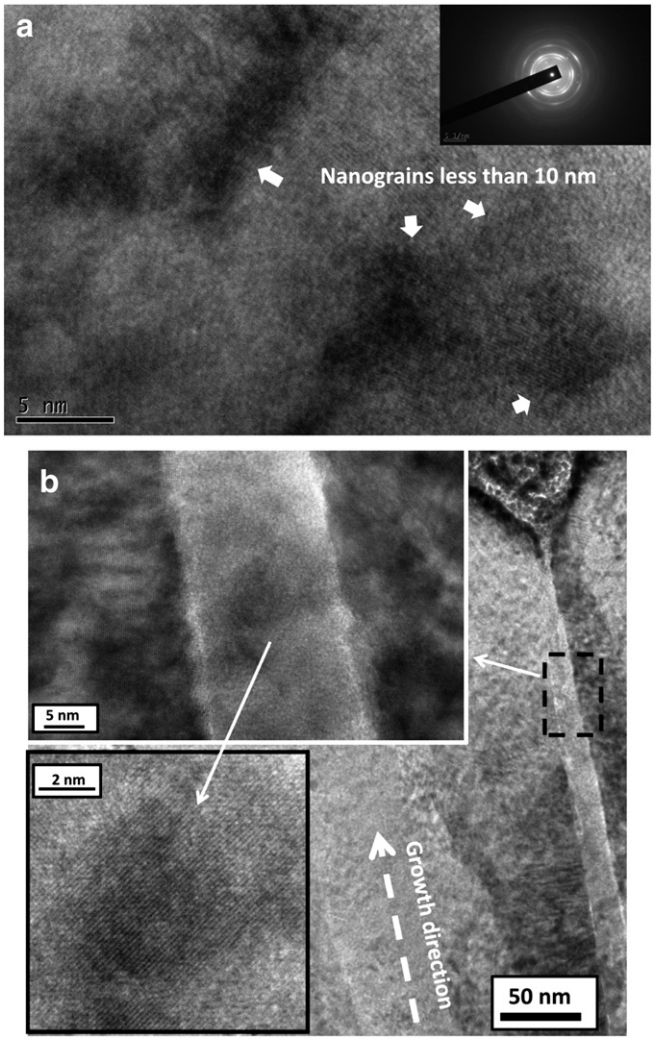

Fig. 5. TEM results of (a) CrAlSiN-4 coating (b) cross-sectional image of upper part of CrAlSiN-GL coating.

3.3. Morphological evolution

Fig. 4 reveals the conversion of microstructure with Si content. For homogeneous structure (through CrAlN to CrAlSiN-4), increasing Si leads the rough columnar structure to smoother less textured and denser structure, in good agreement with literature [4]. This is attributed to the reduced CrAlN grain size as well as the increased amount of amorphous SiN_x phase due to the increased addition of Si. TEM image (Fig. 5(a)) of CrAlSiN-4 further confirms the existence of CrAlN nano-crystallite (less than 10 nm) encapsulated by the amorphous SiN_x phase. Under this condition, SiN_x phase may sever as surface cover layer that partially or completely limited the grain growth periodically, leading to a repeated renucleation and resulting in smaller globular grains which form the dense and less textured structure. However, in graded coatings (CrAlSiN-GL and CrAlSiN-GH) there is no obvious morphological change throughout the coating thickness in the dominant columnar structures. Further examination of this columnar structure of CrAlSiN-GL coating (Fig. 5(b)) reveals the existence of CrAlN nano-grains ~10 nm (as inserted in Fig. 5(b)) in the upper layer (Fig. 5(b)) due to the segregated SiN_x phase as a result of high Si content. The graded coatings have no distinct morphology transition from the bottom to the top in columnar structure, as the initial growth at lower Si addition favor the columnar structure, and afterwards, the increase of Si is gradual.

3.4. Hardness and toughness

The measured hardness is summarized in Table 1. The hardness of homogenous coatings is improved with the increase of Si and the maximum hardness (~29.5 GPa) is achieved at 8.5 at.% Si. This reinforcement could be attributed to the decrease of grain size and the segregated amorphous SiN_x phase. Corresponding reinforced mechanism was discussed by Veprek [17–20]. Graded coatings demonstrate moderate decline in hardness. CrAlSiN-GL exhibits decrease by ~21% as compared to CrAlSiN-3. And ~12% decrease in hardness is observed for CrAlSiN-GH, as compared to CrAlSiN-4.

Scratch test has been employed in estimating coating toughness in addition to adhesion strength [21]. Scratch adhesion strength [14,22] is an easy way to estimate the coating toughness: two representatives load were adopted to describe the failure stages of the hard coatings: i) lower critical load (L_{C1}) at the onset of small trackside buckling and ii) higher critical load (L_{C2}) at the emergence of spallation (total delamination). In other words, the higher the L_{C1}, the more difficult it

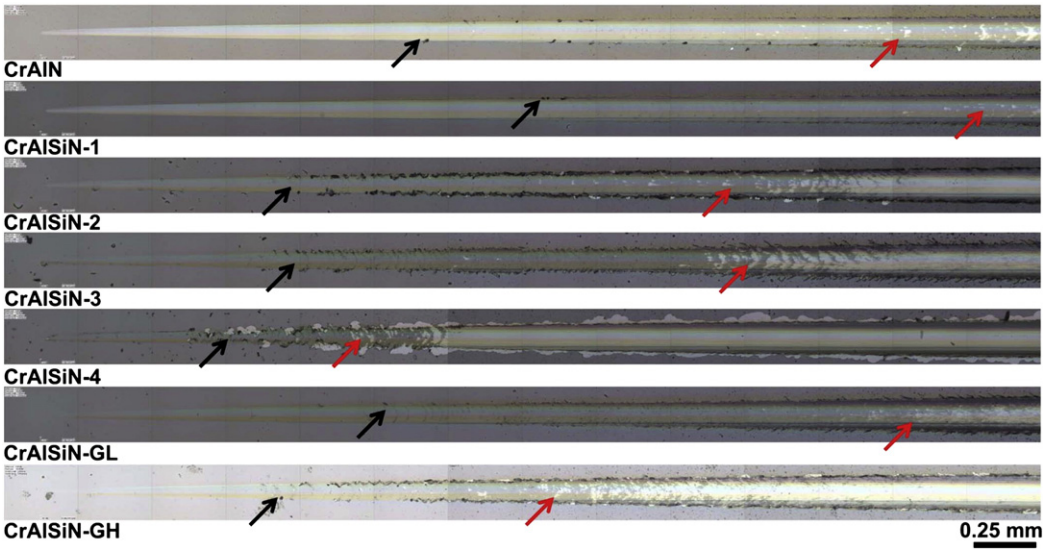

Fig. 6. Optical observation of micro-scratch test of CrAlSiN coatings on SUS420 substrates (black arrow: L_{C1}, red arrow: L_{C2}).

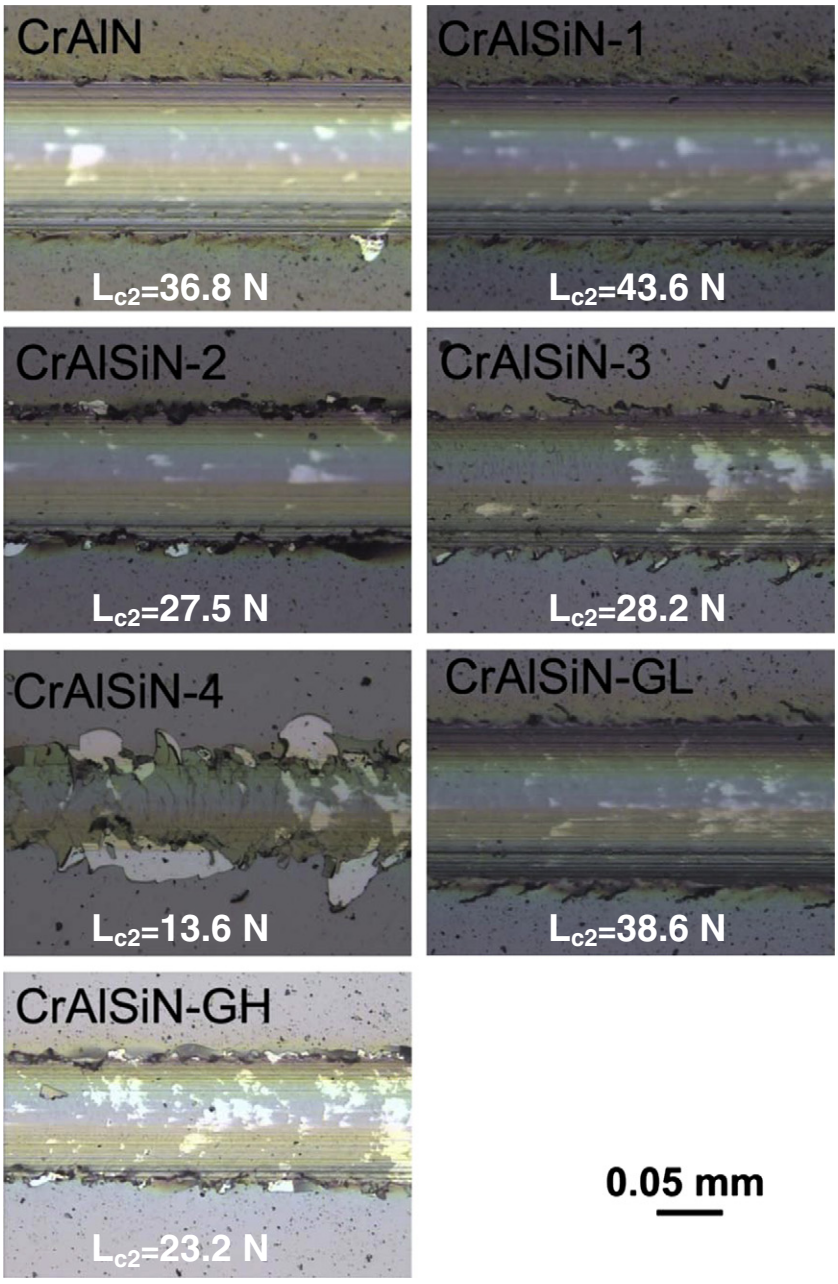

Fig. 7. Fracture behavior at the emergence of spallation.

is to initiate a crack in the coating. And the longer the distance between L_{C1} and L_{C2}, i.e., (L_{C2}–L_{C1}), the more the coating can hold before the catastrophical fracture occurs. Thus the product L_{C1} and (L_{C2}–L_{C1}) is defined as scratch Crack Propagation Resistance (CPR_s) to describe how resistant a coating is to crack propagation under scratch testing. A coating with higher CPR_s will be obviously tougher.

In this study, Si addition in homogenous coatings renders lower L_{C1} (as shown in Fig. 6), indicating increasing brittleness. In particular, severe chipping and buckling occurs at the lowest load ($L_{C1} = 3.69$ N) for CrAlSiN-4. Whereas, the L_{C1} of CrAlSiN-GH with gradient structure is 6.78 N, nearly 80% improvement at an expense of only ~12% in hardness. Enlarged images of failure at L_{C2} are shown in Fig. 7. Cracks in homogenous coatings with lower level of Si are more localized and the graded coatings exhibit good resistance to crack propagation.

The L_{C1} and L_{C2} values are summarized in Table 1, which gives rise to the plot of CPR_s versus hardness (Fig. 8). The measured CPR_s of GH coating is nearly three times as much as that of CrAlSiN-4 coating at the same time maintaining high hardness (25.9 GPa), indicating a fair balance between hardness and toughness. Maintenance of hardness comes from formation of the nanocrystals in the top layer. Great improvement of CPR_s is also observed when comparing CrAlSiN-GL with CrAlSiN-3. This improvement could be attributed to the stress relaxation throughout the coatings as a result of the grading structure, in which the inner rare-Si part plays as softer cushion with more tolerance to the crack propagation while the outer rich-Si layer roles as harder covering maintaining the resistance to the plastic deformation. Therefore, it can be concluded that more Si on the top result the refined nanograins which is responsible for the maintained hardness, while less Si at the bottom is responsible for the good adhesion and improved scratch toughness. Also from Fig. 8, the further research direction is easily seen: to obtain hard yet tough coating, we need to put the data point in the upper right corner in the plot. Looking at the results of the GL and the GH samples, grading of the composition should be in between of that of GL and GH.

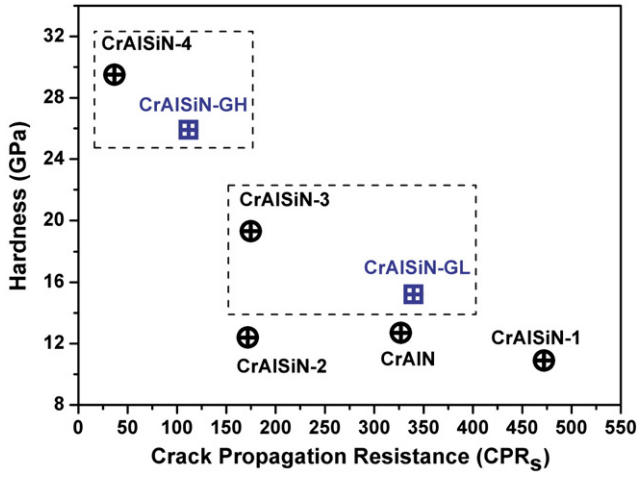

Fig. 8. Scratch crack propagation resistance of as-deposited CrAlSiN coatings on SUS420 substrates.

4. Conclusion

CrAlSiN coatings with gradual increasing of Si along the coating thickness from the coating/substrate interface exhibit high toughness through scratch Crack Propagation Resistance at a slight sacrifice of hardness. The hardness of the homogeneous coating increases with the amount of the silicon incorporation. At lower silicon concentration, the coating is extremely tough with large drop in hardness; at higher silicon concentration, higher hardness is obtained due to formation of silicon rich nanocrystals but sacrificing some toughness. A graded with lower silicon layer at the bottom and higher silicon layer at the top is thus promising as hard yet tough coating for industrial applications.

References

[1] X.-z. Ding, X.T. Zeng, Y.C. Liu, F.Z. Fang, G.C. Lim, Thin Solid Films 516 (2008) 1710.
[2] X.-z. Ding, A.L.K. Tan, X.T. Zeng, C. Wang, T. Yue, C.Q. Sun, Thin Solid Films 516 (2008) 5716.
[3] O. Banakh, P.E. Schmid, R. Sanjinés, F. Lévy, Surf. Coat. Technol. 163–164 (2003) 57.
[4] H.-W. Chen, Y.-C. Chan, J.-W. Lee, J.-G. Duh, Surf. Coat. Technol. 205 (2010) 1189.
[5] H.-W. Chen, Y.-C. Chan, J.-W. Lee, J.-G. Duh, Surf. Coat. Technol. 206 (2011) 1571.
[6] D.B. Lee, T.D. Nguyen, S.K. Kim, Surf. Coat. Technol. 203 (2009) 1199.
[7] C. Ziebert, S. Ulrich, J. Vac. Sci. Technol., A 24 (2006) 554.
[8] S. Zhang, D. Sun, Y. Fu, H. Du, Surf. Coat. Technol. 198 (2005) 2.
[9] U. Helmersson, S. Todorova, S.A. Barnett, J.E. Sundgren, L.C. Markert, J.E. Greene, J. Appl. Phys. 62 (1987) 481.
[10] A. Karimi, Y. Wang, T. Cselle, M. Morstein, Thin Solid Films 420–421 (2002) 275.
[11] J. Lin, J.J. Moore, W.C. Moerbe, M. Pinkas, B. Mishra, G.L. Doll, W.D. Sproul, Int. J. Refract. Met. Hard Mater. 28 (2010) 2.
[12] S. Zhang, X.L. Bui, Y. Fu, D.L. Butler, H. Du, Diam. Relat. Mater. 13 (2004) 867.
[13] S. Zhang, D. Sun, Y. Fu, H. Du, Surf. Coat. Technol. 198 (2005) 74.
[14] S. Zhang, D. Sun, Y. Fu, H. Du, Thin Solid Films 447–448 (2004) 462.
[15] I. Bertóti, Surf. Coat. Technol. 151–152 (2002) 194.
[16] H.C. Barshilia, B. Deepthi, K.S. Rajam, Surf. Coat. Technol. 201 (2007) 9468.
[17] S. Veprek, R.F. Zhang, M.G.J. Veprek-Heijman, S.H. Sheng, A.S. Argon, Surf. Coat. Technol. 204 (2010) 1898.
[18] S. Veprek, M.G.J. Veprek-Heijman, Surf. Coat. Technol. 201 (2007) 6064.
[19] S. Veprek, M.G.J. Veprek-Heijman, P. Karvankova, J. Prochazka, Thin Solid Films 476 (2005) 1.
[20] S. Veprek, A.S. Argon, J. Vac. Sci. Technol. B 20 (2002) 650.
[21] J. Chen, S.J. Bull, J. Phys. D 44 (2011).
[22] J.A. Toque, M.K. Herliansyah, M. Hamdi, A. Ide-Ektessabi, I. Sopyan, J. Vac. Sci. Technol. B 3 (2010) 324.